A&A 537, A73 (2012)
DOI: 10.1051/0004-6361/201118142

Astronomy & Astrophysics

5–14 μm *Spitzer* spectra of Themis family asteroids

J. Licandro[1,2], K. Hargrove[3], M. Kelley[4], H. Campins[3], J. Ziffer[5], V. Alí-Lagoa[1,2], Y. Fernández[3], and A. Rivkin[6]

[1] Instituto de Astrofísica de Canarias, c/Vía Láctea s/n, 38200 La Laguna, Tenerife, Spain
e-mail: jlicandr@iac.es
[2] Departamento de Astrofísica, Universidad de La Laguna, 38205 La Laguna, Tenerife, Spain
[3] Physics Department, University of Central Florida, Orlando, FL 32816, USA
[4] Department of Astronomy, University of Maryland, College Park, MD 20742-2421, USA
[5] University of Southern Maine, Department of Physics, Portland, Maine 04104, USA
[6] Johns Hopkins University Applied Physics Laboratory, Laurel, Maryland 20723, USA

Received 23 September 2011 / Accepted 2 November 2011

ABSTRACT

Context. The Themis collisional family is one of the largest and best established families in the main belt. Composed of primitive asteroids, there is evidence that water is likely present in a large fraction of its members, either in aqueously altered silicates or in water ice reservoirs. The study of the abundance of water in the outer asteroid belt is important as it may be linked to the origin of Earth's water. Studying the Themis family can also help to constrain the compositional and thermal environment in the region of the solar nebula where these asteroids formed.
Aims. Our aim is to constrain the composition and thermal properties of the surfaces of several Themis family asteroids.
Methods. We present 5–14 μm spectra of 8 Themis family asteroids observed with *Spitzer*: (222) Lucia, (223) Rosa, (316) Goberta, (383) Janina, (468) Lina, (492) Gismonda, (515) Athalia, and (526) Jena. We determine their diameters, geometric albedos and beaming parameters using the near-Earth asteroid thermal model. Their emissivity spectra are studied in order to determine if they exhibit an emission plateau from 9 to 12 μm which has been observed in other primitive asteroids and attributed to fine-grained silicates (the Si-O stretch fundamental).
Results. The derived mean albedo of our sample of Themis family asteroids is $\bar{p}_V = 0.07 \pm 0.02$, and the mean beaming parameter is $\bar{\eta} = 1.05 \pm 0.10$. The derived $\bar{\eta}$ value is close to unity, which implies that the infrared beaming is not significant, there is likely little night-side emission from the asteroids, and the thermal inertia is probably low. The emissivity spectra of at least 5 of our 8 asteroids show a 9–12 μm emission plateau with spectral contrast of ~2–4%, similar but smaller than that observed in the spectra of Trojan asteroids and cometary dust. The plateau may be due to the surfaces having either small silicate grains embedded in a relatively transparent matrix, or from a very under-dense (fairy-castle) surface structure.
Conclusions. The surfaces of a large fraction of Themis family asteroids with $D \sim 50$ km are covered by a fine grained silicate mantle as observed on Trojan asteroids of similar or larger size. The lower amplitude of the silicate emission in Themis family asteroids spectra (2–4%) with respect to that of Trojan asteroids (10–15%) could be attributed to larger dust particles, a slightly denser structure, or a lower silicate dust fraction.

Key words. minor planets, asteroids: general – methods: observational – techniques: spectroscopic – infrared: planetary systems – minor planets, asteroids: individual: Themis

1. Introduction

With more than 1600 members, the Themis family (as defined by Zappalà 1995) is the fourth most numerous main-belt asteroid family, one of the more statistically reliable ones (Mothé-Diniz et al. 2005), and one of the oldest (2.5 Gy old, Nesvorný et al. 2008). Located in the outer main belt, its closeness to the 2/1 mean motion resonance with Jupiter – the Hecuba gap (near 3.3 AU) – suggests that the catastrophic event that formed the family also populated the resonant zone (Morbidelli et al. 1995, 2002). The objects were swept off this region, creating the gap and spreading members of this family to other regions of the asteroid belt. However, this family is not believed to be an important contributor to the near-Earth asteroid population (Morbidelli et al. 2002).

The study of Themis family asteroids provides information about the interior of their parent body (e.g., Cellino et al. 2002; Carvano et al. 2003). Moreover, studies of primitive (non-igneous) asteroid families can help constrain the compositional and thermal environment in the region of the solar nebula where these asteroids formed providing clues to the compositional and thermal history in this area of the solar system. The present distribution of water and hydrated minerals in our solar system is very relevant to understanding how it formed and evolved. Water is widespread in the outer solar system and scarce or absent among the inner planets; however, its abundance in the outer asteroid belt is not well defined (e.g., Rivkin et al. 2002; Emery & Brown 2003). The abundance of water and hydrated minerals in this region of the asteroid belt may be linked to the origin of Earth's water (Drake & Campins 2006; Campins & Drake 2010).

Themis family asteroids are compositionally primitive, mainly members of the C-complex in the Tholen classification system (e.g., Mothé-Diniz et al. 2005; Florczak et al. 1999). Ziffer et al. (2011) presented near-infrared spectroscopy in the 0.8–2.5 μm region and found reasonable matches between the spectra of the observed asteroids and the spectra of some carbonaceous chondrite meteorites.

Spectral studies over the visible and 2.5 to 4.0 micron region indicate that water is present in a large fraction of Themis family

Table 1. Observational circumstances of the observations.

Object	Date	r	δ	α	Exp. time (s)
(222) Lucia	2008-Dec.-09	3.503	3.26	16.83	365.7–37.7
(223) Rosa	2008-Sep.-10	3.437	2.896	–15.86	88.1–37.7
(316) Goberta	2008-Sep.-11	3.628	3.256	–15.97	365.7–37.7
(383) Janina	2008-Nov.-28	2.933	2.41	–18.96	88.1–37.7
(468) Lina	2008-Jul.-10	3.625	3.053	–14.51	117.4–37.7
(492) Gismonda	2008-Dec.-15	3.518	3.49	16.69	365.7–37.7
(515) Athalia	2009-Jan.-08	2.66	2.013	19.38	37.7–37.7
(526) Jena	2009-Mar.-04	2.876	2.833	20.25	88.1–37.7

Notes. r is the heliocentric distance in AU, δ is the asteroid – *Spitzer* distance in AU, *alpha* is the phase angle in degrees (Sun – asteroid – *Spitzer*, a negative phase angle indicates that the observation occurred before opposition), and *exp.time* is the total "on object" exposure time in the SL2 and SL1 modes respectively.

asteroids. For example, a 0.49–0.92 μm spectroscopic study of 36 Themis family members, by Florczak et al. (1999), found evidence of aqueous alteration in ~50% of their sample. A compositional heterogeneity among the family members is evident from the taxonomy; of the 37 Themis asteroids that have been classified, 6 are C-type, 17 B-type, 5 Ch-type, 8 Cb-type, 5 X-type, 1 Xc-type and 1 Xk-type in the Bus classification (Mothé-Diniz et al. 2005), indicating also that not all of the Themis family members are aqueously altered. Water-ice was found on the surface of the largest member of the family, (24) Themis (Campins et al. 2010; Rivkin & Emery 2010), using 3-μm spectroscopy. Also at least two smaller members, 133P/Elst-Pizarro and 176P/LINEAR, present cometary-like activity (Hsieh et al. 2006; Licandro et al. 2011) likely induced by water-ice sublimation. We note that 133P is also a member of the newly discovered Beagle family (Nesvorný et al. 2008). So water-ice has likely survived in the interior of some of these asteroids since their formation. Hsieh & Jewitt (2006) postulated that the heating event that produced the aqueous alteration did not affect the whole parent body, and pockets of water ice remained in the fragments borne of the large collision that formed the family. The observed spectral variability between the members of the Themis family supports the view that the parent body was thermally altered, and the distribution of compositions can be attributed to fragments coming from different parts of the original parent body that, according to Castillo-Rogez & Schmidt (2010), could be differentiated into a rocky core and an icy shell at the time of the break-up.

In this paper, we present 5–14 μm mid-infrared spectral data of 8 Themis-family asteroids. The data were obtained with the NASA *Spitzer* Space Telescope. The primary goal of our observations is to characterize the surface compositions and physical properties. In Sect. 2 we present the observations and data reduction. In Sect. 3 we present the results (diameters, geometric albedos and beaming parameters) obtained by fitting the observations with a thermal model, and compare them with previous results on those objets and on other relevant populations. In Sect. 4 we present the derived emissivity spectra and derive information about the composition of the surface of these asteroids, and in Sect. 5 we present our conclusions.

2. *Spitzer* mid infrared spectra

Spectra of the asteroids were obtained with the Infrared Spectrograph (IRS) instrument (Houck et al. 2004) on NASA's *Spitzer* Space Telescope (Werner et al. 2004) between Sept. 2008 and March 2009 (see Table 1 for details on the dates and observational circumstances). The IRS measures spectra over the range 5.2–38 μm with several different configurations. The observations presented here used two segments of the low spectral resolution mode ($R = \lambda/\Delta\lambda \sim 64-128$). These two segments are short wavelength, 2nd order (SL2; 5.2 to 7.6 μm) and short wavelength, 1st order (SL1; 7.4 to 14.2 μm). When the slit of one of the low-resolution orders is centered on the target, the other is offset (~50″) from the target, providing a measurement of the sky background. Our analysis is limited to wavelengths <13.2 μm to avoid a known artifact in IRS spectra at 13.2–14 μm (the 14 μm "teardrop").

Our reduction begins with the basic calibrated data from the *Spitzer* Science Center's IRS reduction pipeline version S18.7.0. We subtract background from and mask the bad pixels in the images, then extract spectra using the SPICE (*Spitzer* IRS Custom Extraction) software, using the default point source-tuned aperture. We scaled the SL2 spectra to match the SL1 spectra at 7.5 μm. The scale factors obtained (between 0.906 and 1.006) are consistent with the IRS pipeline's absolute calibration uncertainty of ≤10%. When reporting values that depend on the absolute calibration (e.g., thermal emission model parameters), we will include an additional 10% flux uncertainty added in quadrature. The flux density spectra of the asteroids are plotted in Fig. 1 along with the best-fit thermal models (see Sect. 3).

3. Thermal model

The flux from these asteroids in the 5–14 μm range is dominated by thermal emission. According to Campins et al. (2009), "The measured spectral energy distribution (SED) depends on the object's size, composition, and temperature distribution. This last term is dependent on several factors, including distance from the Sun, albedo, thermal inertia, surface roughness, rotation rate, shape, and spin-pole orientation". We used a relatively simple near-Earth asteroid thermal model – Near-Earth Asteroid Thermal Model (NEATM, Harris 1998), described below – to fit the 5 to 13 μm spectra.

The NEATM is a refinement of the standard thermal model (STM, Lebofsky et al. 1986, Lebofsky & Spencer 1989), which was developed and calibrated for main-belt asteroids. Unlike the STM, the NEATM requires observations at multiple wavelengths and uses this information to force the model temperature distribution to be consistent with the apparent color temperature of the asteroid. The NEATM solves simultaneously for the beaming parameter (η) and the diameter (D). The beaming parameter was originally introduced in the STM to allow the model temperature distribution to fit the observed enhancement of thermal emission at small solar phase angles due to surface roughness. In practice, η can be thought of as a modeling parameter that allows

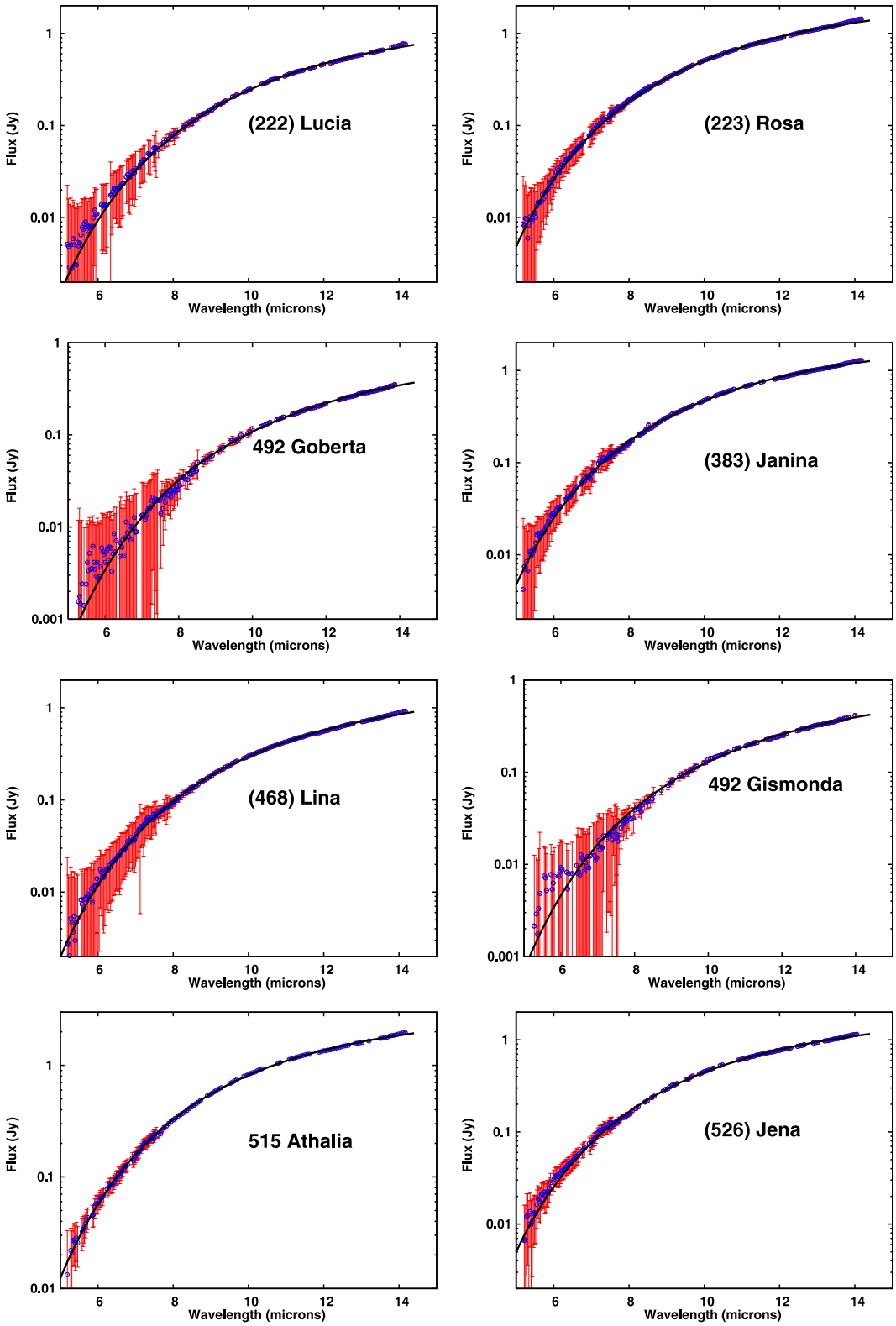

Fig. 1. Flux density spectra of the 8 observed Themis family asteroids in the mid-infrared (circles) and best-fit NEATM (blue solid line). The NEATM fits are done using wavelengths <13.2 μm to avoid a known artifact in IRS spectra at longer wavelengths.

a first-order correction for any effect that influences the observed surface temperature distribution (such as beaming, thermal inertia, and rotation).

Using the NEATM (with bolometric emissivity 0.9) we derived D and η. Those best-fitting models are shown in Fig. 1. We did not make any observations of these asteroids' reflected-sunlight continuum below 2 μm, so to estimate the visible geometric albedos (p_V), we made use of the absolute magnitude (H_V) and the best-fit D (via the standard formula $D = 10^{-H/5}(1329\ \mathrm{km}/\sqrt{p_V})$). The values for H_V were retrieved from the JPL Small-Body Database Browser (`http://ssd.jpl.nasa.gov/`). All our results are presented

Table 2. Derived physical properties for the 8 Themis asteroids we observed.

Object	D(km)	p_V	η	H_V	A(mag)	D_{IRAS}(km)	p_V(IRAS)
(222) Lucia	59.8 ± 0.8	0.110	1.03 ± 0.02	9.13	0.25–0.33	54.66 ± 3.9	0.132 ± 0.021
(223) Rosa	61.2 ± 0.3	0.063	0.85 ± 0.01	9.68	0.06	87.61 ± 4.4	0.031 ± 0.003
(316) Goberta	46.8 ± 1.2	0.097	1.15 ± 0.04	9.80	0.20–0.27	47.92 ± 1.9	0.093 ± 0.008
(383) Janina	48.4 ± 0.3	0.082	1.12 ± 0.01	9.91	0.17	45.52 ± 1.8	0.093 ± 0.008
(468) Lina	59.7 ± 0.5	0.058	0.95 ± 0.01	9.83	0.10–0.18	69.34 ± 2.5	0.043 ± 0.003
(492) Gismonda	50.3 ± 1.1	0.084	1.12 ± 0.03	9.80	0.10	51.69 ± 1.4	0.080 ± 0.005
(515) Athalia	43.0 ± 0.2	0.031	1.07 ± 0.01	11.23	···	38.22 ± 2.1	0.039 ± 0.005
(526) Jena	52.3 ± 0.5	0.055	1.10 ± 0.02	10.17	0.27–0.35	41.49 ± 2.0	0.088 ± 0.009

Notes. Diameter D, albedo p_V and beaming parameter η were determined using NEATM, the absolute magnitude H_V was taken from the JPL Small-Body Database Browser, visual light-curve amplitude A was taken from Harris et al. (2011), and D_{IRAS} and p_V(IRAS) are the diameter and albedo reported using IRAS (Tedesco et al. 2002). Albedo uncertainties are not quoted since they depend on the light curve amplitudes and on the unreported uncertainties in H_V.

in Table 2. Note that the listed uncertainty in the derived diameters and beaming parameters is determined by the uncertainty of the thermal fluxes. However, the true uncertainty relies in the shape and rotational context of each asteroid, which have amplitudes as listed in Table 2. This uncertainty also dominates the uncertainty on the derived albedos.

3.1. Comparison with IRAS results

Thermal observations of these Themis family asteroids obtained with IRAS have been published by Tedesco et al. (2002). Their diameter and albedo determinations are also included in Table 2 for comparison purposes. The diameters determined in this work and those by IRAS are significantly different (differences larger than 3σ) only in the case of asteroids (223) Rosa, (468) Lina, and (526) Jena. Notice anyway that in Tedesco et al. (2002) the model used to fit IRAS fluxes assume $\eta = 0.756$ and this could explain the differences. For example, in the case of (526) Jena, Ryan & Woodward (2010) revisited IRAS observations and using NEATM determined $D = 46.173 \pm 1.727$ km, which is within 3σ of our determination. The results presented in this paper are computed using a much better dataset, a better model, and derive diameters and albedos that are compatible with previous results.

3.2. Albedo and η distribution of Themis family asteroids

We note that the asteroids presented in this paper lie in a very narrow range of diameters from 43 to 61 km. Care is therefore required when extrapolating the derived thermal properties to the whole family, as albedo and beaming parameter can be size dependent.

The derived mean albedo of our sample of Themis family asteroids is $\bar{p}_V = 0.07 \pm 0.02$, typical of primitive asteroids (e.g. Hsieh et al. 2009 and references therein). The mean of the beaming parameter is $\bar{\eta} = 1.05 \pm 0.10$, where the quoted uncertainty is the error in the mean not the standard deviation. This $\bar{\eta}$ value (close to unity) suggests that infrared beaming is not significant, there is little night-side emission from the asteroid, and that the thermal inertia is low, as expected for asteroids covered by a fine-grained regolith.

3.3. Comparison with possibly related small body populations

We will first compare our results with the known thermal properties of MBCs. Licandro et al. (2011) show that MBCs 133P/Elst-Pizarro and 176P/LINEAR should be considered Themis family asteroids not only because of dynamical considerations but also because their reflectance spectra are very similar to those of other Themis-family members. Hsieh et al. (2009) obtained the size and albedo of these two MBCs using *Spitzer* photometry at 24 μm. Assuming $\eta = 1.0$, they obtained $D = 3.8 \pm 0.3$ km and $p_R = 0.05 \pm 0.02$ for 133P and $D = 4.0 \pm 0.2$ km and $p_R = 0.06 \pm 0.02$ for 176P. Our results also support their conclusion that 133P and 176P albedos are typical of Themis family asteroids. This also suggests that small Themis family asteroids like 133P and 176P have similar thermal properties as objects that are one order of magnitude larger in diameter.

Next we compare our results with the thermal properties of Jupiter family comets (JFCs) in order to explore any possible link between both populations. Themis family asteroids are low albedo objects like JFCs, but some of the Themis asteroids in this paper have an albedo value larger than the upper limit $p_R = 0.075$ as suggested by Fernández et al. (2005). On the other hand, the mean $\bar{\eta}$ of the Themis family asteroids presented here is similar to the $\bar{\eta} = 1.03 \pm 0.11$ value reported for JFCs by Fernández et al. (2011).

Finally, our derived η distribution of Themis family asteroids is also similar to the $\bar{\eta} = 1.07 \pm 0.27$ obtained for a large set of main belt asteroids of different spectral types by Ryan & Woodward (2010). Ryan & Woodward conclude that beaming parameter is independent of asteroid composition, as they obtained identical $\bar{\eta}$ for S- and C-type asteroids. Note that the error in the $\bar{\eta}$ we obtain for our 8 Themis family asteroids (0.10) is much smaller, which indicates that our targets have a narrower η distribution. However, our sample is small and a larger dataset is needed to obtain more robust results.

4. The emissivity spectra

Emissivity spectra of the 8 Themis family asteroids were obtained by dividing each asteroid's flux density spectrum by the best-fitting thermal model (see Fig. 2). An emission plateau at about 9 to 12 μm is clearly present in the resulting emissivity spectra of 5 asteroids: (383) Janina, (468) Lina, (492) Gismonda, (515) Athalia and (526) Jena. The plateau has a spectral contrast of ~2–4%. This plateau is not so clearly defined in the spectra of (222) Lucia, and (316) Goberta and not seen in the spectrum of (223) Rosa. This emission bands are evidently due to the Si-O stretch fundamental and thus indicative of silicates.

In order to verify that the spectral features observed in our targets are not observational artifacts, we examined IRS SL calibration sources in the *Spitzer* archive. As an example,

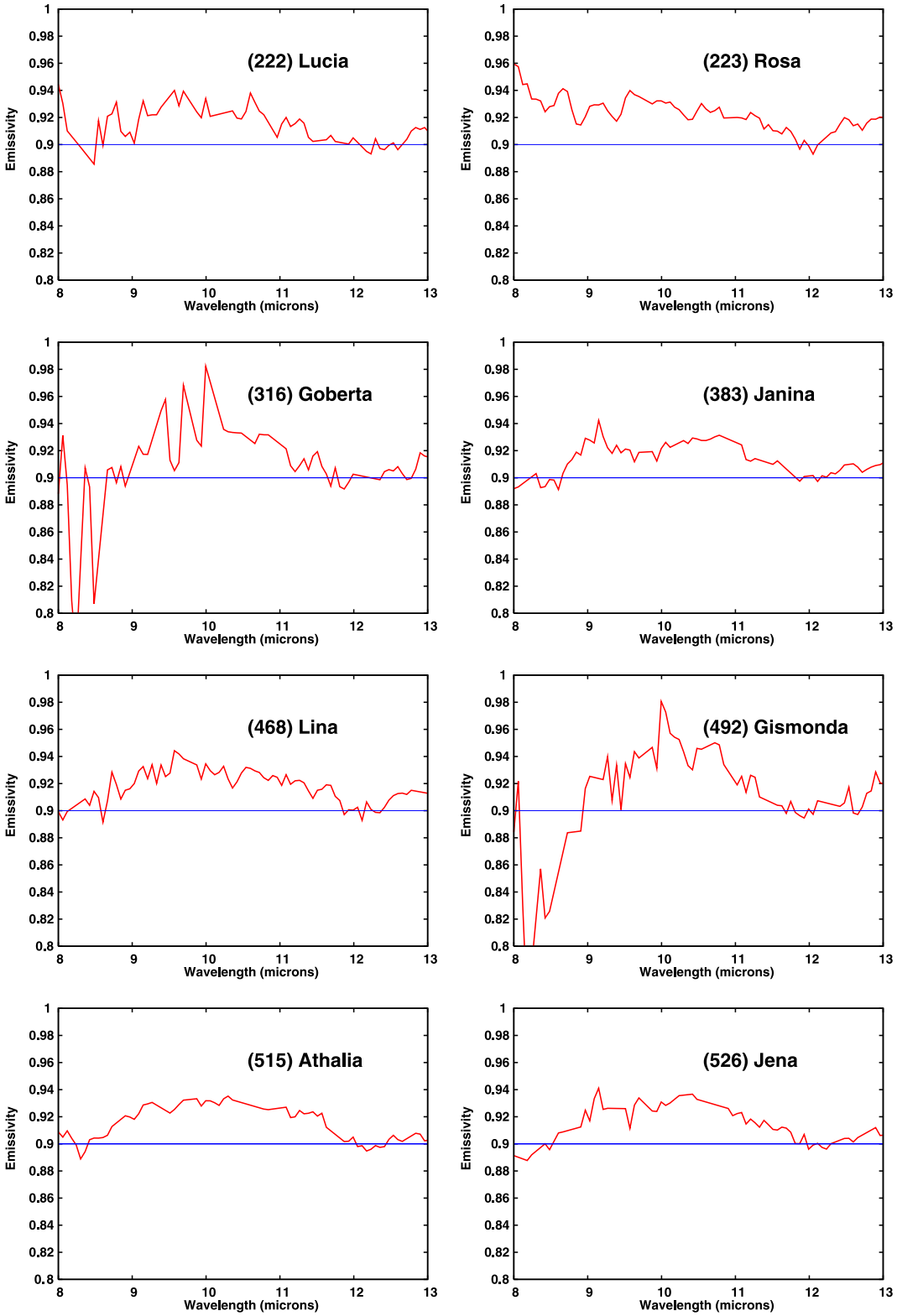

Fig. 2. Emissivity spectra of the 8 observed Themis family asteroids. Notice the emission plateau from 9 to 12 μm with a spectral contrast of ~2–4% that is present in at least five (383 Janina, 468 Lina, 492 Gismonda, 515 Athalia and 526 Jena) and possibly seven (222 Lucia and 316 Goberta) of them.

we downloaded and reduced the 5–13 μm spectra of 6 standard stars from IRS observing campaign 54, the same campaign that included our (223) Rosa and (316) Goberta observations. The data reduction methods are identical to those of our program targets. The extracted spectra are normalized with the spectral templates provided by the *Spitzer* Science Center[1]; several of those templates are described by Decin et al. (2004). The

[1] Available at `http://irsa.ipac.caltech.edu/data/SPITZER/docs/irs/`

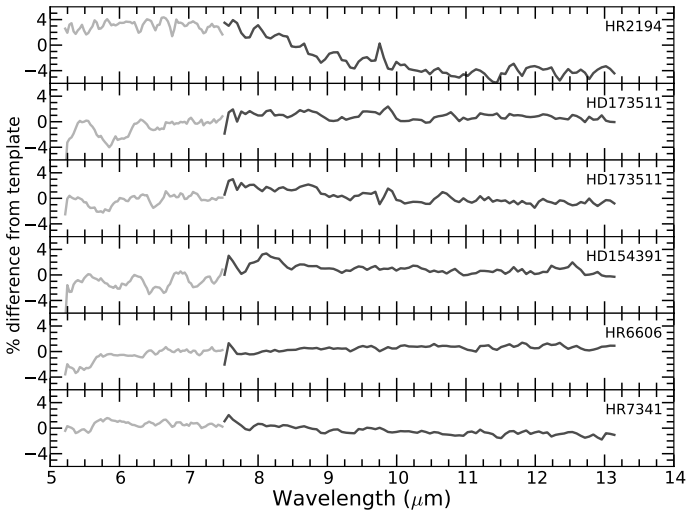

Fig. 3. Spectra of 6 standard stars from IRS observing campaign 54 reduced in the same way as the asteroid spectra and normalized with the spectral templates. Notice that the residual features are smaller than the spectral features observed in our target asteroids (see text).

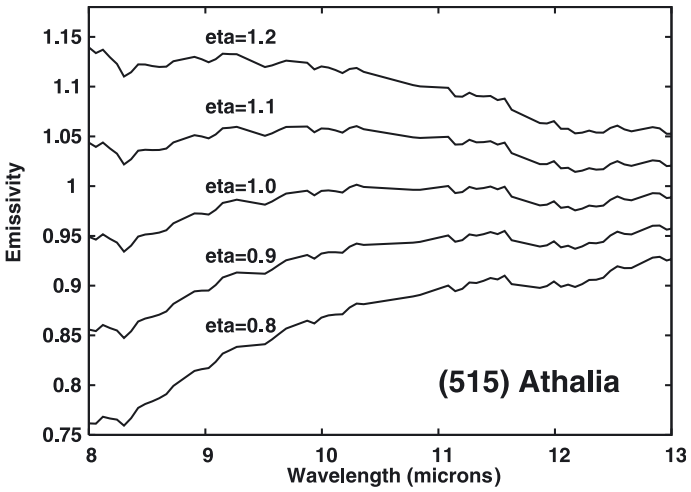

Fig. 4. Emissivity spectra of (515) Athalia obtained from the flux density spectrum by using a best-fit NEATM with a series of fixed η values. Spectra are shifted in emissivity by 0.04 for clarity. The spectrum computed using $\eta = 0.8$ remains unshifted. Notice that the emission plateau is present in all spectra which demonstrate that this is not dependent on the validity of the thermal model.

resulting normalized spectra are shown in Fig. 3. Although there are residual features apparent at the 1–2% level in the standard stars, they are not consistent from source-to-source and would not produce the 2–4% features in the 9 to 12 μm range necessary to explain our asteroid spectra.

To demonstrate that the observed emission plateau is independent of the validity of the thermal model, we computed the NEATM for five different fixed η values (η = 0.8, 0.9, 1.0, 1.1, 1.2) that would best fit the flux density spectrum of (515) Athalia. We then obtained the emissivity spectra, as described above; these are shown in Fig. 4. Notice that the main difference between the spectra is just in the slope (and that the spectrum for η = 1.1 is very similar to Athalia's spectrum in Fig. 2 that uses η = 1.07). Importantly, the plateau is present in all cases, showing that this does not depend on the NEATM fit.

The spectra of other primitive asteroids – i.e. three Trojans presented by Emery et al. (2006) and (65) Cybele presented by

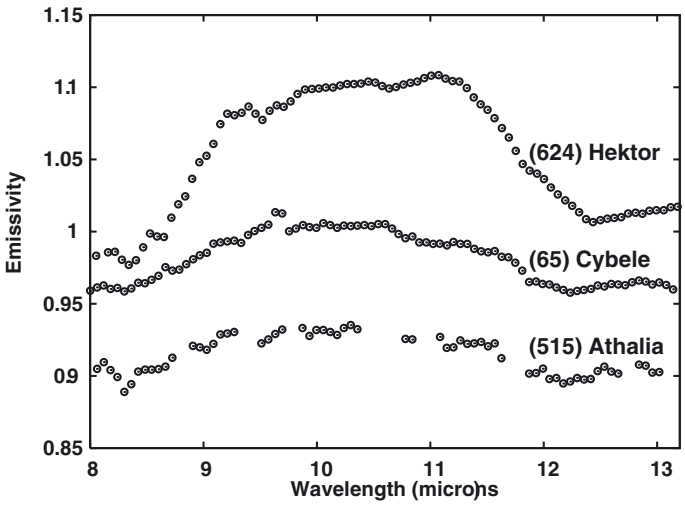

Fig. 5. Emissivity spectrum of (515) Athalia, compared to those of (65) Cybele and Trojan asteroid (624) Hektor (shifted in the emissivity axis for clarity). Notice the emission plateau due to fine-grained silicates in the spectra of the three asteroids. Also note that the contrast is smaller (~3–4%) in the spectrum of (515) Athalia than in that of (65) Cybele (~ 5%) and in that of Hektor (~15%).

Licandro et al. (2011) – also show a similar emission plateau but with higher contrast: 10 to 15% in the case of Trojans, and 5% in the case of (65) Cybele. To illustrate that, the emissivity spectrum of (515) Athalia is plotted in Fig. 5 together with that of Trojan asteroid (624) Hektor (from Emery et al. 2006) and (65) Cybele (from Licandro et al. 2011).

Emery et al. (2006) present an extensive comparison of their Trojans' spectra with that of different kinds of silicates and meteorite samples and with cometary dust comae, and conclude that fine-grained silicates, and no other mineral group, reproduce the major features of the spectra. They argue that the emissivity spectra more closely resemble the emission spectra from cometary comae than those from solid surfaces and those measured in the laboratory for powdered meteorites and regolith analogs. They also hypothesize that the coma-like emission from the solid surfaces of Trojans may be due to small silicate grains being embedded in a relatively transparent matrix, or due to a very under-dense ("fairy-castle") surface structure. Another source for the emission features could be the electrostatic levitation of small particles above the surface (Lee 1996), thus producing a dispersed medium. In any case, we conclude from this and from the fact that we see emission bands in most (5 to 7) of our 8 asteroids that a significant fraction of large ($D \sim 50$ km) Themis family asteroids have a surface covered by a mantle of fine dust grains. The lower amplitude of the silicate emission in our spectra and in (65) Cybele's spectrum – compared to that in the Trojan asteroid spectra – can be attributed to larger dust particles, a slightly denser structure, and/or a lower silicate dust fraction on the surfaces as compared to what is on the surface of the Trojans studied by Emery et al.

5. Summary and conclusions

We presented 5–14 μm spectra of 8 Themis family asteroids obtained with the Infrared Spectrograph (IRS) instrument on NASA's *Spitzer* Space Telescope. We derived their diameters, geometric albedos and beaming parameters using the NEATM, and also obtained their emissivity spectra.

The derived mean albedo of our sample of Themis family asteroids is $\bar{p}_V = 0.07 \pm 0.02$, a low albedo typical of primitive

asteroids (e.g. Hsieh et al. 2009 and references therein), and the mean beaming parameter is $\bar{\eta} = 1.05 \pm 0.10$. As $\bar{\eta}$ value is close to unity, the infrared beaming is not significant, there is likely little night-side emission from the asteroid, and the thermal inertia is probably low, which is compatible with a surface covered with fine regolith. These results also support the conclusion of Hsieh et al. (2009) that the albedos of MBCs 133P/Elst-Pizarro and 176P/LINEAR ($p_R = 0.05 \pm 0.02$ and 0.06 ± 0.02 respectively) are typical of Themis family asteroids and support the conclusion of Licandro et al. (2011) that this objects are likely activated members of the family.

The emissivity spectrum in the 5–14 μm spectral range of a large fraction of the observed Themis family asteroids exhibit an emission plateau at about 9 to 12 μm with a spectral contrast of ~2–4%, similar to that observed in Trojan asteroids (Emery et al. 2006; Mueller et al. 2010) and in (65) Cybele (Licandro et al. 2011). The emission is attributed to small silicate grains being embedded in a relatively transparent matrix, or to a very underdense (fairy-castle) surface structure. Alternatively, electrostatic levitation of small particles above the surface can produce a dispersed medium. These interpretations of the emissivity plateau are compatible with the conclusion from the calculated spectra that the thermal inertia is low. The lower amplitude of the silicate emission in the Themis-family spectra and the Cybele spectrum – compared to that of Trojan asteroids – can be attributed to larger dust particles, to a slightly denser structure, and/or to a lower silicate dust fraction.

Finally, considering that: (i) asteroid (24) Themis has water-ice on its surface (Campins et al. 2010; Rivkin & Emery 2010) and that other Themis family asteroids present comet-like activity (Hsieh & Jewitt 2006; Licandro et al. 2011), which suggest that water ice is still present in several Themis family members; (ii) comet nuclei develop dust mantles as a consequence of the sublimation of their ices; then, the presence of a dust mantle on the surface of several of the Themis family asteroid presented here is consistent with past water ice sublimation.

Acknowledgements. We thank Josh Emery for his useful comments on the manuscript. We thank M. Delbó for providing the NEATM code used in this work. J.L. gratefully acknowledges support from the spanish "Ministerio de Ciencia e Innovación" (MICINN) project AYA2008-06202-C03-02. H. Campins acknowledges support from NASA and the National Science Foundation. This work is based on observations made with the *Spitzer* Space Telescope, which is operated by the Jet Propulsion Laboratory, California Institute of Technology under a contract with NASA. Support for this work was provided by NASA through an award issued by JPL/Caltech.

References

Campins, H., & Drake, M. 2010, in Water & life: the unique properties of H20, ed. R. Lynden-Bell, et al. (CRC Press), 221
Campins, H., Emery, J., Kelley, M., et al. 2009, A&A, 503, 17
Campins, H., Hargrove, K., Pinilla-Alonso, N., et al. 2010, Nature, 464, 1320
Carvano, J. M., Mothé-Diniz, T., & Lazzaro, D. 2003, Icarus, 161, 356
Castillo-Rogez, J., & Schmidt, B. 2010, Geophys. Res. Lett., 37, L10202
Cellino, A., Bus, S. J., Doressoundiram, A., & Lazzaro, D. 2002, in Asteroids III, ed. W. F. Jr. Bottke, A. Cellino, P. Paolicchi, & R. P. Binzel (Tucson: University of Arizona Press), 633
Decin, L., Morris, P. W., Appleton, P. N., et al. 2004, ApJSS, 154, 408
Drake, M. J., & Campins, H. 2006,in Asteroids, Comets and Meteorites, ed. D. Lazzaro et al. (Cambridge Univ. Press), 381
Emery, J. P., Cruikshank, D. P., & van Cleve, J. 2006, Icarus, 182, 496
Fernández, Y., Jewitt, D., & Sheppard, S. 2005, AJ, 130, 308
Fernández, Y., Kelley, M. S., Lamy, P., et al. 2011, A&A, submited
Florczak, M., Lazzaro, D., Mothé-Diniz, T., et al. 1999, A&ASS, 134, 463
Harris. A. W. 1998, Icarus, 131, 291
Harris, A. W., Warner, B. D., & Pravec, P. 2011, Asteroid Lightcurve Derived Data V12.0. EAR-A-5-DDR-DERIVED-LIGHTCURVE-V12.0. NASA Planetary Data System
Houck, J. R., Roelling, T. L., van Cleave, J., et al. 2004, ApJSS, 154, 18
Hsieh, H., & Jewitt, D. 2006, Science, 312, 561
Hsieh, H., Jewitt, D., & Fernández, Y. 2009, ApJ, 694, 111
Lee, P. 1996, Icarus, 124, 181
Lebofsky, L. A., & Spencer, J. R. 1989, in Asteroids II, ed. R. P. Binzel, T. Gehrels, & M. S. Matthews (Tucson: Univ. of Arizona Press), 128
Lebofsky, L. A., Sykes, M. V., Tedesco, E. F., et al. 1986, Icarus, 68, 239
Licandro, J., Campins, H., Tozzi, G. P., et al. 2011, A&A, 532, 35
Morbidelli, A., Zappalà, V., Moons, M., Cellino, A., & Gonczi, R. 1995, Icarus, 118, 132
Morbidelli, A., Jedicke, R., Bottke, W. F., Michel, P., & Tedesco, E. F. 2002, Icarus, 158, 329
Mothé-Diniz, T., Roig, F., & Carvano, J. M. 2005, Icarus, 174, 54
Mueller, M., Marchis, F., Emery, J., et al. 2010, Icarus, 205, 505
Nesvorný , D., Bottke, W. F., Levison, H. F., & Dones, L. 2003, ApJ, 591, 486
Nesvorny, D., Bottke, W. F., Vokrouhlický, D., et al. 2008, ApJ, 679, L143
Rivkin, A. S., & Emery, J. 2010, Nature, 464, 1322
Rivkin, A. S., Howell, E. S., Vilas, F., & Lebofsky, L. A. 2002, in Asteroids III, ed. W. F. Bottke, A. Cellino, P. Paolicchi, & R. P. Binzel (Univ. Arizona Press), 235
Rivkin, A. S., Davies, J., Johnson, J., et al. 2003, Meteorit. Planet. Sci., 38, 1383
Ryan, E. L., & Woodward, C. E. 2010, AJ, 140, 933
Tedesco, E. F., Noah, P. V., Noah, M., & Price, S. D. 2002, AJ, 123, 1056
Werner, M. W., Roelling, T. L., Low, F. J., et al. 2004, ApJSS, 154, 1
Zappalà, V., Bendjoya, P., Cellino, A., Farinella, P., & Froeschle, C. 1995, Icarus, 116, 291
Ziffer, J., Campins, H., Licandro, J., et al. 2011, Icarus, 213, 538